

Multiparticle Exciton Ionization in Shallow Doped Carbon Nanotubes

Jay D. Sau,^{*,†} Jared J. Crochet,^{*,‡} Stephen K. Doorn,[¶] and Marvin L. Cohen^{§,⊥}

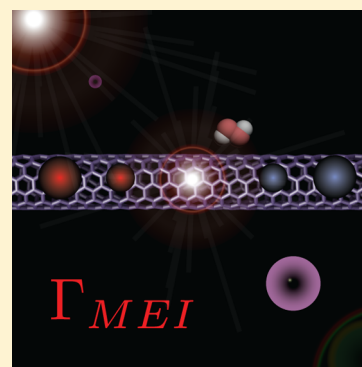
[†]Department of Physics, Harvard University, Cambridge, Massachusetts, United States

[‡]Physical Chemistry and Applied Spectroscopy and [¶]Center for Integrated Nanotechnologies, Los Alamos National Laboratory, Los Alamos, New Mexico, United States

[§]Department of Physics, University of California at Berkeley, Berkeley, California, United States

[⊥]Materials Sciences Division, Lawrence Berkeley National Laboratory, Berkeley, California, United States

ABSTRACT: Shallow hole doping in small-diameter semiconducting carbon nanotubes with a valley degeneracy is predicted to result in the resonant ionization of excitons into free electron–hole pairs. This mechanism, which relies on the chirality of the electronic states, causes excitons to decay with high efficiencies where the rate scales as the square of the dopant density. Moreover, multiparticle exciton ionization can account for delocalized fluorescence quenching when a few holes per micrometer of tube length are present.



SECTION: Spectroscopy, Photochemistry, and Excited States

For more than a decade, single-walled carbon nanotubes (SWNTs) have shown unique transport, optical, and mechanical properties, making them one of the most promising systems for nanotechnology applications. The optical properties of SWNTs have proven to be particularly intriguing because they are dominated by strong resonances associated with bound excitons. In particular, the GW-Bethe–Salpeter formalism^{1,2} for understanding the optical properties of semiconductors has been applied with great success to understanding the positions of the peaks in the absorption spectrum of SWNTs.^{3–5} Apart from the absorption frequency spectrum, the exciton lifetime also plays a critical role in determining the light emission efficiency of carbon nanotubes for optical devices. As a result, there have been several studies, both theoretical^{6–8} and experimental, on the lifetimes of excitons.^{9,10}

An examination of these studies reveals certain discrepancies between theory and experiment, leading to the conclusion that the important problem of exciton decay is not understood. The most fundamental exciton lifetime mechanism for optically active excitons is radiative decay.⁶ However, the calculated radiative decay lifetime is found to be on the order of a few nanoseconds as opposed to experimentally measured lifetimes of a few tens of picoseconds.^{11,12} Moreover, experimentally, it is found that only about 1% of the decay of excitons is radiative, ruling light emission out as a dominant mechanism.¹³ In order to account for low emission efficiencies, it has been shown that excitons can be highly mobile along the tube backbone, with diffusion lengths that can be hundreds of nanometers,^{12,14–21} resulting in a large probability that an exciton will encounter the tube end or a quenching defect within its lifetime. Besides low emission

efficiencies because of high exciton mobilities, carbon nanotubes have also been found to be hole-doped spontaneously by the presence of the aqueous oxygen redox couple,²² molecular oxygen,²³ and other redox species such as H₂O₂.^{20,24} Therefore, alternative decay mechanisms involving Auger decay with a free hole⁸ as well as a phonon-assisted process⁷ have been proposed to account for chemically induced nonradiative decay channels.

We propose an ionization mechanism for the decay of excitons into free electron–hole pairs, which is purely a result of the Coulomb interaction. This mechanism is unlike the conventional Auger mechanism and leads to the generation of four particles, that is, two electron–hole pairs, instead of a single high-energy hole. This eliminates the kinetic energy barrier involved in the Auger decay and allows the process to occur for zero-momentum bright excitons. The rate of decay from this mechanism is calculated using a two-band model with parameters fit to match prior calculations of excitons supported by experimental results. Our investigation suggests that photoluminescence quenching may occur when only a few holes per micrometer of tube length are present.

In hole-doped SWNTs, photoexcitations can decay by the Auger process where the exciton decays by transferring its energy and momentum to a hole.⁸ However, this mechanism requires the exciton dispersion to intersect with the hole dispersion at an energy comparable to the thermal energy so that both energy and momentum can be conserved. This only leads to an efficient

Received: January 8, 2013

Accepted: March 5, 2013

Published: March 5, 2013

decay mechanism of dark excitons,⁸ which have a larger effective mass than the holes. Therefore, the conventional Auger mechanism does not lead to decay of the zero-momentum bright excitons that are created by the incident radiation. The other mechanism that has been suggested for the decay of excitons in doped carbon nanotubes is the phonon-assisted indirect exciton ionization (PAIEI) mechanism.⁷ Here, the phonon provides the excess momentum needed for the dissociation process. However, for low dopant densities, the PAIEI mechanism leads to a lifetime that is too long to be consistent with experiment,²⁰ and in the high doping regime, metallic screening may dominate and lead to bleaching of transitions.²⁵

Given that the currently studied mechanisms are unable to account satisfactorily for exciton dissociation in the low doping regime, we consider a four-particle mechanism outlined in Figure 1, where we define a multiparticle exciton ionization (MEI). In chiral carbon nanotubes, the electronic states arise from a mirror symmetry of the K/K' valleys associated with the underlying

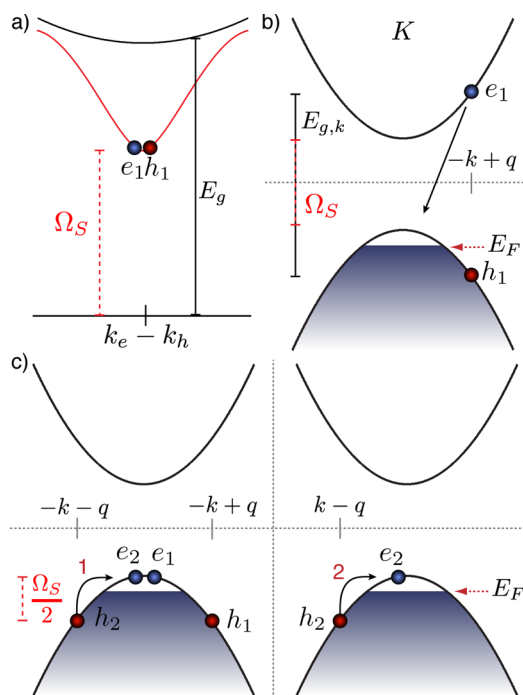


Figure 1. (a) Exciton dispersions for a bright exciton (red line) and the free electron-hole pair continuum (black line) in semiconducting carbon nanotubes. Ω_S is the exciton energy, and E_g is the free electron-hole pair gap where the exciton binding energy is given by $E_b = \Omega_S - E_g$. (b) Initial state of an electron-hole pair in the K valley, near $k_{eh} \approx 0$, that makes up the bright exciton in (a). The arrow illustrates the initial scattering of e_1 in a slightly doped SWNT with a hole pocket in the otherwise filled valence band. The filled part of the valence band is shaded blue, where E_F is the Fermi level. The exciton instantaneously at one possible center of mass momentum in the K valley is composed of the vertically separated electron-hole pair, e_1 and h_1 , in the K valley. (c) The final state where e_1 nonradiatively decays from the conduction band $\epsilon_{e,k}$ into the hole pocket near $-k$, leaving the hole h_1 at $-k + q$. At the same time, another electron e_2 makes a transition from the filled valence state at $-k - q$ to the hole pocket near $-k$ to conserve energy and momentum in the K valley. This is an intravalley process denoted as 1. Alternatively, e_2 makes a transition from the filled valence state at $k - q$ to the hole pocket near k to conserve energy and momentum in the K' valley. This is an intervalley process denoted as 2. Energy is conserved as the final electron-hole pairs have a total energy of Ω_S .

graphene sublattices, which are energetically degenerate and have opposite angular momentum on the quantized tube. Here, an electron from an exciton makes a transition to the hole pocket, defined by the Fermi momentum $k_F = \pi n_d/4$, where n_d is the linear dopant density, in the K valley while another electron makes a transition from the occupied valence band into the hole pocket in the K' valley. In Figure 1b, E_F refers to the Fermi level associated with the filled Fermi sea, shown as the shaded region. Excitations above the Fermi sea are referred to as electrons, while those below the Fermi sea are referred to as holes, and the phrase hole pocket refers to the part of the valence band above E_F that supports electron-like excitations. The resulting process is a decay of the exciton into a pair of electrons in the hole pocket together with a pair of holes in the occupied valence band. The interaction driving this scattering process is the screened Coulomb interaction of the semiconducting tube.²⁶ We are assuming that we are at sufficiently low doping, $k_F \approx 10^{-2} \rightarrow 10^{-4} \text{ nm}^{-1}$, so that the metallic screening can be ignored.²⁵ Therefore, we take the Coulomb interaction to be in the static limit, and the calculated decay rate of the exciton is related to the strength of the screened Coulomb interaction, which in turn will be estimated from the exciton binding energy.

The initial exciton state with center of mass momentum K_0 in the single band approximation can be written as

$$|\Psi_{\text{exc},K_0}\rangle = \int dq dr_e dr_h A_{c,v,K_0} \phi_{c,q+(K_0/2)}(r_e) \phi_{v,q-(K_0/2)}^*(r_h) c^\dagger(r_e) c(r_h) |0\rangle \quad (1)$$

where $\phi_{(c,v),k'}$ are the conduction and valence band wave functions for the carbon nanotube and c^\dagger is the electron creation operator on the lattice of carbon atoms on the nanotube acting on the vacuum state $|0\rangle$.²⁷ Note that the vacuum state $|0\rangle$ already contains a hole pocket, so that the hole creation operator $\phi_{v,k_1=q-(K_0/2)}(r) c(r_h) |0\rangle$ must vanish for k_1 in the hole pocket. Strictly speaking, this implies that the corresponding Bethe-Salpeter equation for the exciton wave function $A_{c,v,k'}$ must be viewed as a variational problem with the constraint that $A_{c,v,k'}$ vanishes whenever $q \pm (K_0/2)$ is in the hole pocket. However, for the small sizes of the hole pocket considered here, this constraint can be neglected.

The wave functions ϕ , $A_{c,v,k'}$, and the exciton energy Ω_S have been obtained previously from first-principles calculations.¹⁻³ Therefore, the exciton decay into multiquasiparticle states is obtained by considering the Coulomb interaction perturbatively on the exciton. The lowest-order Coulomb interaction processes where an exciton decays into hole quasiparticles is shown in Figure 1c. In terms of the state $|0\rangle$, the final state with a pair of electrons at k_{e1}, k_{e2} both in the hole pocket and a pair of holes at k_{h1}, k_{h2} in the occupied part of the valence band can be written as

$$|k_{e1}, k_{e2}, k_{h1}, k_{h2}\rangle = \int dr_{e1} dr_{e2} dr_{h1} dr_{h2} \phi_{vk_{e1}}(r_{e1}) \phi_{vk_{e2}}(r_{e2}) \phi_{vk_{h1}}^*(r_{h1}) \phi_{vk_{h2}}^*(r_{h2}) c^\dagger(r_{e1}) c^\dagger(r_{e2}) c(r_{h1}) c(r_{h2}) |0\rangle \quad (2)$$

As in the case of eq 1, the above definition of states only applies to the wave vectors k_{h1}, k_{h2} being outside of the hole pocket and vanishes when either of these wave vectors is in the hole pocket. For small sizes of the hole pocket, the phase space corresponding to final states with these vanishing states, which must be excluded, is small and may be ignored. The final multiple

quasiparticle states must continue to have a center of mass momentum $k_{e_1} + k_{e_2} - k_{h_1} - k_{h_2} = K_0$ and also a total energy equal to the excitation energy $\varepsilon_v(k_{e_1}) + \varepsilon_v(k_{e_2}) - \varepsilon_v(k_{h_1}) - \varepsilon_v(k_{h_2}) = \Omega_S$ of the exciton, Figure 1. Here, $\varepsilon_v(k)$ is the valence band dispersion of the highest valence band of the nanotube. Neglecting the Fermi energies of the hole pocket (i.e., $|\varepsilon_v(k_{e_1})|, |\varepsilon_v(k_{e_2})| \ll \Omega_S$), the final hole energies can be approximated by $\Omega_S \approx -(\varepsilon_v(k_{h_1}) + \varepsilon_v(k_{h_2}))$. Because the thermal energy of the exciton is much lower than Ω_S (so that $K_0 \ll |k_{h_1}|, |k_{h_2}|$), we can further approximate $\varepsilon_v(k_{h_1}) \approx \varepsilon_v(k_{h_2}) \approx -\Omega_S/2$ and $k_{h_1} \approx -k_{h_2}$. Furthermore in Figure 1, only states in the exciton in eq 1 where the hole momentum q equals the final hole momentum $q = k_{h_2}$ contribute to the decay process.

Including spin and valley degeneracy, there are a total of 12 processes in a chiral tube, 6 which are shown in Figure 2, related

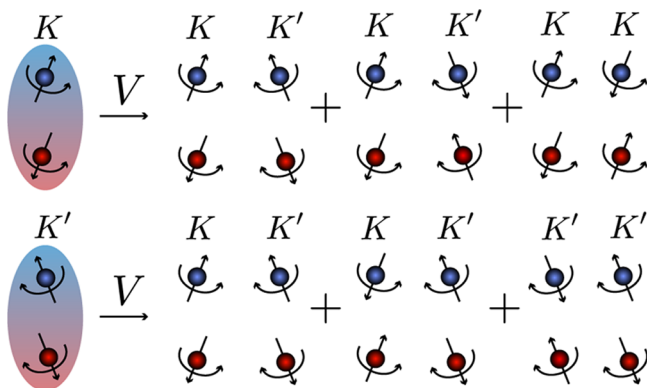


Figure 2. Schematic of the spin and valley degrees of freedom involved in the proposed decay mechanism, where the spin is given by the straight line and the valley by a curved line. An exciton at K or K' , given by the shaded oval, can decay via the Coulomb interaction V into two electron–hole pairs in the three spin–valley configurations shown. Similarly, the spin-opposite configuration of these process can happen, giving a total of 12 possible decay channels.

by particle exchange to obtain the same final state starting from the exciton. All of these processes are mediated by the screened Coulomb interaction.²⁶ Because $k_{e_1} \approx k_{e_2}$ are in the hole pocket and are small, spin is not conserved when an electron–hole pair is created in the same valley with the same spin configuration of the exciton. Therefore, we only consider the cases where the exciton scatters into an electron–hole pair in the same valley with an equal or opposite spin configuration while the other electron–hole pair is created in a different valley with an equal or opposite spin configuration or the same valley with an opposite spin configuration. Here, we assume that e_1 and h_1 arise from the exciton and that an Auger process creates the pair e_2 and h_2 , and we are in a low doping regime such that exciton binding energies or band gaps are unperturbed. We can then assume $k_{e_1}, k_{e_2} \approx k_F \ll q$, and the decay rate using Fermi's golden rule is written as

$$\Gamma_{\text{MEI}} = \frac{24\pi k_F^2}{\hbar} \int dq |M(q)|^2 D(q) \quad (3)$$

where the matrix element $M(q) = \langle \Psi_{\text{exc}} | V | (h, 0), (h, 0); (h, -q), (h, q) \rangle$ and the density of free electron–hole pair states (including spin and valley degeneracy) in the k - p approximation is given by $D(q) = 4(\hbar v_F |q|)^{-1} (q^2 + k_x^2)^{1/2}$. Using the exciton wave

function $A(q)$ and the Coulomb interaction $V(q)$, the square of the matrix element can be expressed as

$$|M(q)|^2 = \frac{q^2}{4(q^2 + k_x^2)} A^2(q) V^2(q) \quad (4)$$

where the e–h pair wave function overlaps $|\langle u_{e,-q} | u_{h,0} \rangle|^2 |\langle u_{h,q} | u_{h,0} \rangle|^2 = (1/4) q^2 / (q^2 + k_x^2)$ have been used from the k - p approximation.⁵

Given the small doping levels of the nanotube, we will restrict ourselves to a simplistic two-band continuum model⁵ to estimate Γ_{MEI} . Within this approximation, the screened electron–hole interaction is taken to be of the form $V(q) = gU(|q/k_x|) = gI_0(|q/k_x|)K_0(|q/k_x|)$, where I_0 and K_0 are Bessel functions and g is a coupling constant. Here, $k_x = 2/(3d)$ is the transverse momentum quantum for the electrons on the nanotube, which defines the free particle gap $E_g = 2\hbar v_F k_x$, where d is the diameter of the nanotube. The two-band continuum Bethe–Salpeter equation can be written in dimensionless form as

$$(\sqrt{1 + \tilde{k}^2} - 1 - \varepsilon) B(\tilde{k}) = \lambda \int d\tilde{q} U(\tilde{q}) F(\tilde{k}; \tilde{k} + \tilde{q}) B(\tilde{k} + \tilde{q}) \quad (5)$$

where the rescaled coupling constant is $\lambda = gk_x/E_g$, the dimensionless exciton binding energy is $\varepsilon = E_b/E_g$, and $\tilde{k} = k/k_x$ and $\tilde{q} = q/k_x$. Here, the chirality factor

$$F(k_1; k_2) = \frac{1}{2} \left[1 + \frac{1 + k_1 k_2 / k_x^2}{\sqrt{1 + k_1^2 / k_x^2} \sqrt{1 + k_2^2 / k_x^2}} \right] \quad (6)$$

arises from the overlaps $|\langle u_{e,k} | u_{e,k_1} \rangle| |\langle u_{h,k} | u_{h,k_1} \rangle|$ in the k - p theory, and we have used $\Omega_S = E_g + E_b$, with $E_b < 0$. Moreover, it is clear from the left-hand side of eq 5 that energy conservation requires that $(1 + \tilde{k}^2)^{1/2} - 1 = \varepsilon$, which gives the phase space restriction $\tilde{k} = [\varepsilon(\varepsilon + 2)]^{1/2}$. Similar to the Bethe–Salpeter equation, we recast the decay rate in eq 3 using the above-defined nondimensional quantities such that

$$\Gamma_{\text{MEI}} = \frac{9d\pi^3 n_d^2 \lambda^2 v_F |\tilde{k}| B(\tilde{k})^2 U(\tilde{k})^2}{\sqrt{\tilde{k}^2 + 1}} \quad (7)$$

In order to estimate Γ_{MEI} , the dimensionless solution $B(\tilde{k})$ to the exciton wave function and ε are obtained from previous calculations for the screened Coulomb interactions in nanotubes.⁷ We find that for an effective dielectric constant of $\kappa = 3.3$, $B(\tilde{k}) \approx (1 + 1.69\tilde{k}^2)^{-1.3}$ and $\varepsilon \approx -0.23$. This value of ε suggests that $E_b \approx -0.23E_g$ or for the prototypical (6,5) tube, $E_b \approx -370$ meV for $E_g \approx 1.6$ eV, which is consistent with experimental estimates.²⁸ Integrating both sides of eq 5 over \tilde{k} , we obtain $\lambda = 0.35$, which varies less than 10% upon changing the integration range from $\tilde{k} = 2$ to 20.

Given the coupling constant λ and \tilde{k} , eq 7 can be simplified to

$$\Gamma_{\text{MEI}} \approx v_F n_d^2 d \quad (8)$$

which is valid in the low doping regime ($n_d \approx < 10 \mu\text{m}^{-1}$) where dynamical screening of the Coulomb interaction is predicted to lead to small changes in the exciton binding energy.²⁵ This equation is the central result of our analysis, and we point out that the rate scales as n_d^2 as compared to n_d in the PAIEI mechanism.⁷ In order to compare this result to similar exciton–exciton annihilation processes in a tube of length L , we define an Auger constant such that $A = v_F d/L$. For a small-diameter nanotube,

such as the (6,5) tube with $d = 0.75$ nm, with an energy gap within $k \cdot p$ of $E_g = 2\hbar v_F k_x = 1.6$ eV, the Fermi velocity should be $v_F \approx 1.36$ nm \cdot fs $^{-1}$. Therefore, for a single hole dopant in a 1 μ m tube, $A \approx 1$ nm \cdot ps $^{-1}$, which is nearly 3 orders of magnitude smaller than estimations of similar exciton–exciton annihilation processes.²⁹ This is easily understood from the phase space restriction, outlined above, arising from energy conservation. However, when compared to a phonon-assisted process (PAIEI), Figure 3a, we find that MEI is much more efficient. In fact, for a single hole dopant in a 1 μ m tube, MEI is approximately 80% more efficient than PAIEI.

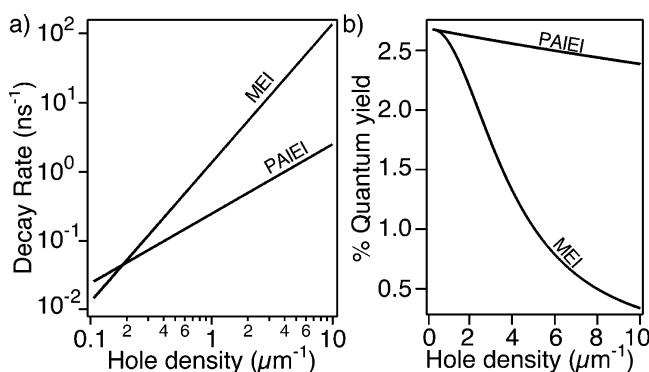


Figure 3. (a) Calculated decay rates for both the PAIEI⁷ and MEI (eq 7) mechanisms. (b) Calculated relative fluorescence quantum yields η for the PAIEI⁷ and MEI mechanisms as a function of hole density.

We now estimate the impacts of this model on fluorescence quantum yields in nanotubes assuming no prior doping. Using eq 8 with the standard definition of the fluorescence quantum yield

$$\eta = \frac{\Gamma_r}{\Gamma_r + \Gamma_{nr} + \Gamma_{MEI}} \quad (9)$$

where Γ_r is the radiative decay rate and Γ_{nr} is the nonradiative rate before hole doping, we show a strong change in η as a function of n_d in Figure 3b for MEI as compared to that for the PAIEI mechanism.⁷ Here, $\Gamma_r = 5.5 \times 10^{-4}$ ps $^{-1}$ and $\Gamma_{nr} = 2 \times 10^{-2}$ ps $^{-1}$ are taken from experimental results on undoped (6,5) tubes.^{21,30} Our model suggests that a few holes per micrometer of tube length are sufficient to reduce the fluorescence quantum yield by detectable amounts. Specifically, for a (6,5) tube with an estimated $\eta \approx 2.7\%$, one hole every $d_q \approx 260$ nm could result in $\eta = 1.35\%$. However, excitons in carbon nanotubes are highly mobile, and by including an exciton diffusion length of $l_D \approx 200$ nm,²¹ which is neglected in the above formalism, this quenching range could be extended to approximately $2l_D + d_q \approx 660$ nm, resulting in the same η reduction. Therefore, this model suggests that the multiparticle exciton ionization may be the dominant mechanism of excitonic decay in shallow, doped, small-diameter carbon nanotubes. Supporting our model, single nanotube investigations by Heller et al.²⁴ have demonstrated that single reducing events within 900 nm of the tube length can quench photoluminescence by $\sim 10\%$. Similarly, Crochet et al.²⁰ have shown in long (6,5) tubes that reduction events can quench fluorescence over micrometers of tube length. Such multiparticle states can be expected to relax to the ground state by diffusion-limited recombination processes that would result in power law ground-state recovery kinetics.

In summary, we have demonstrated that excitons can be effectively ionized in small-diameter SWNTs even at relatively

low dopant concentrations. This extremely efficient mechanism is driven by both the particularly strong Coulomb interaction experienced by charge carriers in quasi-one-dimensional systems and the intrinsic chirality of the underlying graphene sublattice. Also, these results may partially account for the exponential quenching of SWNT emission in field effect transistor devices as a function of gate voltage in the low doping regime.¹⁸ Finally, we emphasize that doping at low levels may be of interest for photovoltaic applications where high exciton ionization rates without the expense of bleaching optical transitions is desired.

AUTHOR INFORMATION

Corresponding Author

*E-mail: jaydsau@physics.harvard.edu (J.D.S.); jcrochet@lanl.gov (J.J.C.).

Notes

The authors declare no competing financial interest.

ACKNOWLEDGMENTS

J.S. thanks the Harvard Quantum Optics Center, JQI-NSF-PFC, DARPA-QUEST, and LPS-NSA, and M.L.C. acknowledges the NSF Grant DMR07-05941 and the Director, Office of Science, Basic Energy Sciences, Materials Sciences and Engineering Division of the U.S. Department of Energy under Contract No. DE-AC02-05CH11231. This work was performed, in part, at the Center for Integrated Nanotechnologies, a U.S. Department of Energy, Office of Basic Energy Sciences user facility and was partially supported by the LANL LDRD program. Los Alamos National Laboratory is operated by Los Alamos National Security, LLC, for the National Nuclear Security Administration of the U.S. Department of Energy under Contract No. DE-AC52-06NA25396.

REFERENCES

- (1) Hybertsen, M. S.; Louie, S. G. Electron Correlation in Semiconductors and Insulators: Band Gaps and Quasiparticle Energies. *Phys. Rev. B* **1986**, *34*, 5390–5413.
- (2) Rohlfing, M.; Louie, S. G. Electron–Hole Excitations and Optical Spectra from First Principles. *Phys. Rev. B* **2000**, *62*, 4927–4944.
- (3) Spataru, C. D.; Ismail-Beigi, S.; Benedict, L. X.; Louie, S. G. Excitonic Effects and Optical Spectra of Single-Walled Carbon Nanotubes. *Phys. Rev. Lett.* **2004**, *92*, 077402.
- (4) Jiang, J.; Saito, R.; Samsonidze, G. G.; Jorio, A.; Chou, S. G.; Dresselhaus, G.; Dresselhaus, M. S. Chirality Dependence of Exciton Effects in Single-Wall Carbon Nanotubes: Tight-Binding Model. *Phys. Rev. B* **2007**, *75*, 035407.
- (5) Ando, T. Excitons in Carbon Nanotubes. *J. Phys. Soc. Jpn.* **1997**, *66*, 1066–1073.
- (6) Spataru, C. D.; Ismail-Beigi, S.; Capaz, R. B.; Louie, S. G. Theory and Ab Initio Calculation of Radiative Lifetime of Excitons in Semiconducting Carbon Nanotubes. *Phys. Rev. Lett.* **2005**, *95*, 247402.
- (7) Perebeinos, V.; Avouris, P. Phonon and Electronic Nonradiative Decay Mechanisms of Excitons in Carbon Nanotubes. *Phys. Rev. Lett.* **2008**, *101*, 057401.
- (8) Kinder, J. M.; Mele, E. J. Nonradiative Recombination of Excitons in Carbon Nanotubes Mediated by Free Charge Carriers. *Phys. Rev. B* **2008**, *78*, 155429.
- (9) Wang, F.; Dukovic, G.; Brus, L. E.; Heinz, T. F. Time-Resolved Fluorescence of Carbon Nanotubes and Its Implication for Radiative Lifetimes. *Phys. Rev. Lett.* **2004**, *92*, 177401.
- (10) Huang, L.; Pedrosa, H. N.; Krauss, T. D. Ultrafast Ground-State Recovery of Single-Walled Carbon Nanotubes. *Phys. Rev. Lett.* **2004**, *93*, 017403.

- (11) Berciaud, S.; Cognet, L.; Lounis, B. Luminescence Decay and the Absorption Cross Section of Individual Single-Walled Carbon Nanotubes. *Phys. Rev. Lett.* **2008**, *101*, 077402.
- (12) Hertel, T.; Himmelein, S.; Ackermann, T.; Stich, D.; Crochet, J. Diffusion Limited Photoluminescence Quantum Yields in 1-D Semiconductors: Single-Wall Carbon Nanotubes. *ACS Nano* **2010**, *4*, 7161–7168.
- (13) Crochet, J.; Clemens, M.; Hertel, T. Quantum Yield Heterogeneities of Aqueous Single-Wall Carbon Nanotube Suspensions. *J. Am. Chem. Soc.* **2007**, *129*, 8058–8059.
- (14) Siitonen, A. J.; Tsybolski, D. A.; Bachilo, S. M.; Weisman, R. B. Surfactant-Dependent Exciton Mobility in Single-Walled Carbon Nanotubes Studied by Single-Molecule Reactions. *Nano Lett.* **2010**, *10*, 1595–1599.
- (15) Moritsubo, S.; et al. Exciton Diffusion in Air-Suspended Single-Walled Carbon Nanotubes. *Phys. Rev. Lett.* **2010**, *104*, 247402.
- (16) Harrah, D. M.; Swan, A. K. The Role of Length and Defects on Optical Quantum Efficiency and Exciton Decay Dynamics in Single-Walled Carbon Nanotubes. *ACS Nano* **2011**, *5*, 647–655.
- (17) Liu, T.; Xiao, Z. Exact and Closed Form Solutions for the Quantum Yield, Exciton Diffusion Length, and Lifetime To Reveal the Universal Behaviors of the Photoluminescence of Defective Single-Walled Carbon Nanotubes. *J. Phys. Chem. C* **2011**, *115*, 16920–16927.
- (18) Yasukochi, S.; Murai, T.; Moritsubo, S.; Shimada, T.; Chiashi, S.; Maruyama, S.; Kato, Y. K. Gate-Induced Blueshift and Quenching of Photoluminescence in Suspended Single-Walled Carbon Nanotubes. *Phys. Rev. B* **2011**, *84*, 121409.
- (19) Xie, J.; Inaba, T.; Sugiyama, R.; Homma, Y. Intrinsic Diffusion Length of Excitons in Long Single-Walled Carbon Nanotubes from Photoluminescence Spectra. *Phys. Rev. B* **2012**, *85*, 085434.
- (20) Crochet, J. J.; Duque, J. G.; Werner, J. H.; Doorn, S. K. Photoluminescence Imaging of Electronic Impurity Induced Exciton Quenching in Single-Wall Carbon Nanotubes. *Nat. Nanotechnol.* **2012**, *7*, 126–132.
- (21) Crochet, J. J.; Duque, J. G.; Werner, J. H.; Lounis, B.; Cognet, L.; Doorn, S. K. Disorder Limited Exciton Transport in Colloidal Single-Wall Carbon Nanotubes. *Nano Lett.* **2012**, *12*, 5091–5096.
- (22) Aguirre, C. M.; Levesque, P. L.; M., P.; F., L.; St-Antoine, B. C.; Desjardins, P.; Martel, M. The Role of the Oxygen/Water Redox Couple in Suppressing Electron Conduction in Field-Effect Transistors. *Adv. Mater.* **2009**, *21*, 3087–3091.
- (23) Yoshikawa, K.; Matsuda, K.; Kanemitsu, Y. Exciton Transport in Suspended Single Carbon Nanotubes Studied by Photoluminescence Imaging Spectroscopy. *J. Phys. Chem. C* **2010**, *114*, 4353–4356.
- (24) Heller, D. A.; Jin, H.; Martinez, B. M.; Patel, D.; Miller, B. M.; Yeung, T.-K.; Jena, P. V.; Hobartner, C.; Ha, T.; Silverman, S. K.; Strano, M. S. Multimodal Optical Sensing and Analyte Specificity Using Single-Walled Carbon Nanotubes. *Nat. Nanotechnol.* **2009**, *4*, 114–120.
- (25) Spataru, C. D.; Léonard, F. Tunable Band Gaps and Excitons in Doped Semiconducting Carbon Nanotubes Made Possible by Acoustic Plasmons. *Phys. Rev. Lett.* **2010**, *104*, 177402.
- (26) Takeshima, M. Role of Dielectric Screening in Auger Recombination in Semiconductors. *Phys. Rev. B* **1982**, *26*, 3192–3202.
- (27) Capaz, R. B.; Spataru, C. D.; Ismail-Beigi, S.; Louie, S. G. Diameter and Chirality Dependence of Exciton Properties in Carbon Nanotubes. *Phys. Rev. B* **2006**, *74*, 121401.
- (28) Maultzsch, J.; Pomraenke, R.; Reich, S.; Chang, E.; Prezzi, D.; Ruini, A.; Molinari, E.; Strano, M. S.; Thomsen, C.; Lienau, C. Exciton Binding Energies in Carbon Nanotubes from Two-Photon Photoluminescence. *Phys. Rev. B* **2005**, *72*, 241402.
- (29) Wang, F.; Wu, Y.; Hybertsen, M. S.; Heinz, T. F. Auger Recombination of Excitons in One-Dimensional Systems. *Phys. Rev. B* **2006**, *73*, 245424.
- (30) Gokus, T.; Cognet, L.; Duque, J. G.; Pasquali, M.; Hartschuh, A.; Lounis, B. Mono- and Biexponential Luminescence Decays of Individual Single-Walled Carbon Nanotubes. *J. Phys. Chem. C* **2010**, *114*, 14025–14028.